Author Manuscript

Author Manuscript

Author Manuscript

Author Manuscript

HHS Public Access

Author manuscript

J Am Chem Soc. Author manuscript; available in PMC 2018 January 12.

Published in final edited form as:

J Am Chem Soc. 2008 October 15; 130(41): 13555–13557. doi:10.1021/ja805683r.

A New Peptide-Based Method for the Design and Synthesis of Nanoparticle Superstructures: Construction of Highly Ordered Gold Nanoparticle Double Helices

Chun-Long Chen[†], **Peijun Zhang**[‡], and **Nathaniel L. Rosi**[†]

[†]Department of Chemistry, University of Pittsburgh, 219 Parkman Avenue

[‡]Department of Structural Biology, University of Pittsburgh School of Medicine, 3501 5th Avenue, Pittsburgh, Pennsylvania 15260

Inorganic nanoparticles are widely considered potential structural and functional building-blocks for new technologically significant materials.[1-5] Many properties of these materials are predicted to depend not only on the size, shape, and composition of the nanoparticle building blocks but also to a large extent on the spatial arrangement of these building blocks with respect to one another within a material.[1,2,5] Recently, significant effort has been directed toward assembling nanoparticles into sophisticated structures.[3,6-20] Examples of some typical methods include colloidal crystallization,[3,6-9] molecular templating strategies,[10-13] or directional assembly of multivalent nanoparticles.[14-18] Despite these advances, assembling nanoparticles into well-defined superstructures amenable to practical use still remains a significant challenge, and the development of more facile and efficient methods for rationally designing and fabricating such structures is critically important for the continued advancement of this area. Here we report a new peptide-based method to address this challenge: a one-pot direct approach that couples peptide self-assembly and peptide-based biomineralization into one simultaneous process. In this method, peptide self-assembly, nucleation and growth of particular nanoparticles, the topology of the resultant nanoparticle superstructure, and the precise stereochemical arrangement of nanoparticles within the structure are programmed by rationally designing specific peptide-conjugates. We demonstrate the utility of this method by preparing an unprecedented left-handed gold nanoparticle double-helical structure. We expect that this assembly strategy will allow for the rational design of a variety of relatively complex nanoparticle superstructures and broaden the scope of “bottom-up” fabrication approaches.

Two research developments contributed to the conception of the methodology reported herein: (1) the study and manipulation of peptide self-assembly[21-24] and (2) the in vitro evolution of specific peptides for mineralizing and recognizing specific inorganic materials.[25-29] The former has become a broad field, and various strategies have emerged that allow for the design of peptide-based supramolecular materials. In some cases, the native secondary structure of the peptides, such as α-helix or β-sheet motifs, strongly impact

Correspondence to: Nathaniel L. Rosi.

Supporting Information Available: Experimental procedures, Figures S1-14, and additional supporting data. This material is available free of charge via the Internet at http://pubs.acs.org.

Author Manuscript Author Manuscript Author Manuscript Author Manuscript

structure formation while in other cases, synthetic modifications to the peptide, such as attachment of organic molecule appendages to the peptide terminus, help promote assembly of certain structures. To date, many ordered peptide assemblies, including some that adopt micellar, vesicular, tubular, helical, or membrane architectures, have been reported.[21-24] The latter development has led to the discovery of numerous oligopeptides that recognize and bind particular inorganic materials in a sequence-specific fashion. For example, peptides that exhibit high binding affinities for gold, silver, zinc sulfide, and other inorganic materials have been identified.[28] In some cases, these peptides play a significant role in controlling the nucleation and growth of particular nanoparticles from precursor salt solutions.[26] In this study we show that these two processes, peptide self-assembly and peptide-based nucleation of discrete nanoparticles, can be coupled to occur simultaneously, resulting in a facile method for controlling the synthesis and hierarchical assembly of nanoparticles.

To demonstrate the feasibility of this method, we began by first attaching small organic molecules to peptide AYSSGAPPMPPF and then investigating the assembly of the resultant peptide-conjugates. AYSSGAPPMPPF, hereafter referred to as PEP_{Au}, was evolved and isolated via phage-display methods to have a high affinity for gold surfaces.[26] In the presence of chloroauric acid and HEPES buffer, PEP_{Au} assists the formation of monodisperse spherical gold nanoparticles through a process that involves both the tyrosine residue and HEPES.[26,30-33] Given the hydrophilic nature of PEP_{Au}, we reasoned that attaching an aliphatic carbon tail to its N-terminus would promote its assembly into various multidimensional supramolecular assemblies, such as 1-D peptide amphiphile structures.[23,34] As a first step in this direction, we coupled succinimide-activated dodecanoic acid to the N-terminus of PEP_{Au} to generate $[C_{11}H_{23}CO]$-PEP_{Au}, or C_{12}–PEP_{Au} (Supporting Information, Figures S1, S2). C_{12}–PEP_{Au} was completely dissolved in 0.1 M HEPES buffer, conditions that allow for both C_{12}–PEP_{Au} self-assembly as well as gold nanoparticle nucleation.[26] To gain insight into the structure of the peptide-amphiphile assembly, we examined the assembled structures using transmission electron microscopy (TEM) and tapping-mode atomic force microscopy (AFM). TEM images (Figure 1a) revealed the presence of uniform individual fibers with micrometer lengths (>4 μm) and narrow (6.1 ± 0.6 nm) widths (Figure S11). Using tapping-mode AFM, we determined that each fiber adopts a twisted-ribbon morphology and that the ribbons appear to twist in a left-handed direction (Figure 1b and Figures S4, S5). The pitch of the twisted-nanoribbon was consistently measured to be 84.1 ± 4.2 nm (Figure 1c and Figures S4, S11). Such uniform peptide-nanoribbons are very unusual. Spectroscopic studies were performed to better understand the structure of the helical fibers. Specifically, we examined the fibers using circular dichroism (CD) spectroscopy (Figure S6) and observed a peak around 227 nm, which could correspond to the signal produced by β-sheet structures.[34] To further probe whether β-sheet formation occurs, we analyzed the assembled species using Fourier transform infrared (FT-IR) spectroscopy (Figure S7). The peak at 3275 cm^{-1} corresponds to the stretching frequency of hydrogen-bonded N–H groups. The amide I band (1626 cm^{-1}) is consistent with β-sheet conformations,[35,36] and the C–H vibration bands at 2918 cm^{-1} and 2850 cm^{-1} indicate ordered packing of the aliphatic chains.[37]

Using the spectroscopic and microscopy data, we arrived at a working model for the structure of the nanoribbon assembly. Our model (Figure 1e) is similar to previously

Author Manuscript Author Manuscript Author Manuscript Author Manuscript

developed models.[23,34] The width of the nanoribbon is spanned by two C_{12}–PEP_{Au} units that interact through their aliphatic tails. Organization of the C_{12}–PEP_{Au} units along the longitudinal axis of the nanoribbon is driven by the formation of parallel β-sheets and favorable hydrophobic interactions between the aliphatic tails. Given that the first four amino acids (AYSS) have a propensity to form β-sheets whereas proline residues do not,[38] we propose that these amino acids (AYSS) participate in β-sheet assembly and also likely impart the left-handed helical twist to the nanoribbon.[22,34] The formation of nanoribbons can be attributed to the fact that the outer two-thirds of the peptide sequence is relatively sterically bulky because of the presence of two proline-proline dimers and one phenylalanine. The steric bulk causes the C_{12}–PEP_{Au} units to assemble into nanoribbon structures rather than condensed tubular micelles, while at the same time PEP_{Au} subunits effectively shield the hydrophobic core of the nanoribbon. This working model is consistent with all of our experimental observations.

To determine whether the above process of peptide self-assembly and the process of PEP_{Au} biomineralization could be coupled into one simultaneous process as a means to design and construct double-helical gold nanoparticle superstructures, solutions of chloroauric acid ($HAuCl_4$) were added to clear HEPES buffer solutions containing C_{12}–PEP_{Au} which were carefully filtered to remove any assembled structures. Immediately after the addition of $HAuCl_4$, TEM samples were prepared and their examination revealed that the C_{12}–PEP_{Au} fibers formed even in the presence of the gold salt (Figure S3). When the solutions were allowed to stand for ~30 min, a small amount of precipitate formed. TEM studies of the precipitate suggested formation of double-helical assemblies comprising uniform discrete spherical gold nanoparticles (Figure 2a-e and Figure S10). A better understanding of the structure of the nanoparticle assemblies was obtained from electron tomographic analysis. A series of tilted images from −70° to +70° with 1° tilt intervals were collected. These tilted projections were aligned and combined computationally to reconstruct a three-dimensional electron density map (tomogram). As illustrated in the tomographic slices (Figure 3a) and in a 3-D surface rendering of the reconstructed density map (Figure 3b), the gold nanoparticle assemblies are left-handed double helices, which is in keeping with the observed chirality of the twisted C_{12}–PEP_{Au} nanoribbons. The measured maximum inner-distance between the particles along the width of the double helix is 6.0 ± 0.8 nm, and the pitch of the double helix is 83.2 ± 4.4 nm (Figure S11). Both distances are consistent with the observed width and pitch of the twisted C_{12}–PEP_{Au} nanoribbons. These observations all indicate that the synthesis of the nanoparticles and the assembly of the nanoribbons are coupled and that the peptide-conjugates successfully control the formation of gold nanoparticle double helices (Figure 3c). The results of control experiments help verify this conclusion. When identical syntheses were performed using unmodified PEP_{Au} instead of C_{12}–PEP_{Au}, dispersed nanoparticles formed (Figure S12), similar to those reported in the literature.[26] Further, to assess the importance of the internal amino acids (AYSS) for directing the assembly of the nanoribbons,[34] we attempted to assemble nanoribbons and synthesize the gold nanoparticle double helices using an amphiphile constructed from the reverse peptide sequence (C_{12}–FPPMPPAGSSYA). Nanoribbons do not form using this amphiphile nor do gold nanoparticle double helices; rather, random gold aggregates are the principle product (Figure S13). Finally, to determine whether the C_{12}–PEP_{Au} nanoribbons could template the

Author Manuscript Author Manuscript Author Manuscript Author Manuscript

assembly of preformed gold nanoparticles, we added citrate-stabilized nanoparticles to HEPES solutions containing C_{12}–PEP_{Au} nanoribbons. In this case, no ordered particle assemblies were observed (Figure S14).

The formation of left-handed gold nanoparticle double helices in a single preparative step exemplifies the utility and power of this methodology. The gold nanoparticles comprising the double helices are monodisperse, with diameters of 8.2 ± 1.0 nm (Figure 2e), which suggests a uniform growth process from initial seeding to termination. In addition, the double helices are highly regular: there are approximately 22 nanoparticles per pitch distance (Figure S11), the edge-to-edge spacing between the nanoparticles is uniform (1.5 ± 0.8 nm; Figure S11), and the length of individual helices extends into the micrometer range. Such structural uniformity is unique, and it will be important for many potential applications, especially those that derive from the plasmonic properties of the nanoparticles.[2,5,39] Finally, we note that spatially complex nanoparticle superstructures exhibiting well-defined stereochemistry, order, and persistence over multiple length scales are very rare, and to our knowledge, rational synthetic methods that allow for their fabrication are equally scarce. We are currently expanding the scope of this methodology by targeting various nanoparticle superstructures via variation of the pendant organic group and by tuning the inorganic composition of the assemblies via selection of particular peptides. Ultimately, we expect that this method will be useful for designing and producing many other target nanoparticle superstructures having properties that depend on both the composition of the organic and inorganic components and their arrangement with respect to one another within the assembled structure.

Supplementary Material

Refer to Web version on PubMed Central for supplementary material.

Acknowledgments

Funding for this work was provided by the University of Pittsburgh. The authors thank the Department of Mechanical Engineering and Materials Science for access to electron microscopy instrumentation and the Petersen Institute for Nanoscience and Engineering (PINSE) for access to AFM instrumentation. They are grateful to the various support services provided by the University of Pittsburgh's Department of Chemistry, including the glass shop, machine shop, and electronics shop. They also acknowledge Dr. David Earl, Daniel Lamont, and Dr. Joel Gillespie for fruitful discussions.

References

1. Alivisatos AP. Science. 1996; 271:933–937.
2. Maier SA, Atwater HA. J Appl Phys. 2005; 98:0111010.
3. Kalsin AM, Fialkowski M, Paszewski M, Smoukov SK, Bishop KJM, Grzybowski BA. Science. 2006; 312:420–424. [PubMed: 16497885]
4. Burda C, Chen XB, Narayanan R, El-Sayed MA. Chem ReV. 2005; 105:1025–1102. [PubMed: 15826010]
5. Tang ZY, Kotov NA. AdV Mater. 2005; 17:951–962.
6. Shevchenko EV, Talapin DV, Kotov NA, O'Brien S, Murray CB. Nature. 2006; 439:55–59. [PubMed: 16397494]
7. Park SY, Lytton-Jean AKR, Lee B, Weigand S, Schatz GC, Mirkin CA. Nature. 2008; 451:553–556. [PubMed: 18235497]

Author Manuscript Author Manuscript Author Manuscript Author Manuscript

8. Nykypanchuk D, Maye MM, van der Lelie D, Gang O. Nature. 2008; 451:549–552. [PubMed: 18235496]
9. Zhuang JQ, Wu HM, Yang YA, Cao YC. J Am Chem Soc. 2007; 129:14166–14167. [PubMed: 17963395]
10. Novak JP, Feldheim DL. J Am Chem Soc. 2000; 122:3979–3980.
11. Boal AK, Ilhan F, DeRouchey JE, Thurn-Albrecht T, Russell TP, Rotello VM. Nature. 2000; 404:746–748. [PubMed: 10783884]
12. Le JD, Pinto Y, Seeman NC, Musier-Forsyth K, Taton TA, Kiehl RA. Nano Lett. 2004; 4:2343–2347.
13. Li M, Schnablegger H, Mann S. Nature. 1999; 402:393–395.
14. Alivisatos AP, Johnsson KP, Peng XG, Wilson TE, Loweth CJ, Bruchez MP, Schultz PG. Nature. 1996; 382:609–611. [PubMed: 8757130]
15. Caswell KK, Wilson JN, Bunz UHF, Murphy CJ. J Am Chem Soc. 2003; 125:13914–13915. [PubMed: 14611200]
16. Zubarev ER, Xu J, Sayyad A, Gibson JD. J Am Chem Soc. 2006; 128:15098–15099. [PubMed: 17117855]
17. Xu XY, Rosi NL, Wang YH, Huo FW, Mirkin CA. J Am Chem Soc. 2006; 128:9286–9287. [PubMed: 16848436]
18. DeVries GA, Brunnbauer M, Hu Y, Jackson AM, Long B, Neltner BT, Uzun O, Wunsch BH, Stellacci F. Science. 2007; 315:358–361. [PubMed: 17234943]
19. Ryadnov MG, Ceyhan B, Niemeyer CM, Woolfson DN. J Am Chem Soc. 2003; 125:9388–9394. [PubMed: 12889969]
20. Stevens MM, Flynn NT, Wang C, Tirrell DA, Langer R. AdV Mater. 2004; 16:915–918.
21. Ulijn RV, Smith AM. Chem Soc ReV. 2008; 37:664–675. [PubMed: 18362975]
22. Aggeli A, Nyrkova IA, Bell M, Harding R, Carrick L, McLeish TCB, Semenov AN, Boden N. Proc Natl Acad Sci US A. 2001; 98:11857–11862.
23. Hartgerink JD, Beniash E, Stupp SI. Science. 2001; 294:1684–1688. [PubMed: 11721046]
24. Zhang SG. Nat Biotechnol. 2003; 21:1171–1178. [PubMed: 14520402]
25. Whaley SR, English DS, Hu EL, Barbara PF, Belcher AM. Nature. 2000; 405:665–668. [PubMed: 10864319]
26. Slocik JM, Stone MO, Naik RR. Small. 2005; 1:1048–1052. [PubMed: 17193392]
27. Tomczak MM, Slocik JM, Stone MO, Naik RR. MRS Bull. 2008; 33:519–523.
28. Sarikaya M, Tamerler C, Jen AKY, Schulten K, Baneyx F. Nat Mater. 2003; 2:577–585. [PubMed: 12951599]
29. Evans JS, Samudrala R, Walsh TR, Oren EE, Tamerler C. MRS Bull. 2008; 33:514–518.
30. Slocik JM, Zabinski JS, Phillips DM, Naik RR. Small. 2008; 4:548–551. [PubMed: 18383577]
31. Si S, Bhattacharjee RR, Banerjee A, Mandal TK. Chems-Eur J. 2006; 12:1256–1265.
32. Habib A, Tabata M, Wu YG. Bull Chem Soc Jpn. 2005; 78:262–269.
33. Xie JP, Lee JY, Wang DIC. Chem Mater. 2007; 19:2823–2830.
34. Paramonov SE, Jun HW, Hartgerink JD. J Am Chem Soc. 2006; 128:7291–7298. [PubMed: 16734483]
35. Surewicz WK, Mantsch HH, Chapman D. Biochemistry. 1993; 32:389–394. [PubMed: 8422346]
36. Georget DMR, Belton PS. Biomacromolecules. 2006; 7:469–475. [PubMed: 16471918]
37. Helmy R, Fadeev AY. Langmuir. 2002; 18:8924–8928.
38. Minor DL, Kim PS. Nature. 1994; 367:660–663. [PubMed: 8107853]
39. Chen Y, Munechika K, Ginger DS. MRS Bull. 2008; 33:536–542.

Author Manuscript Author Manuscript Author Manuscript Author Manuscript

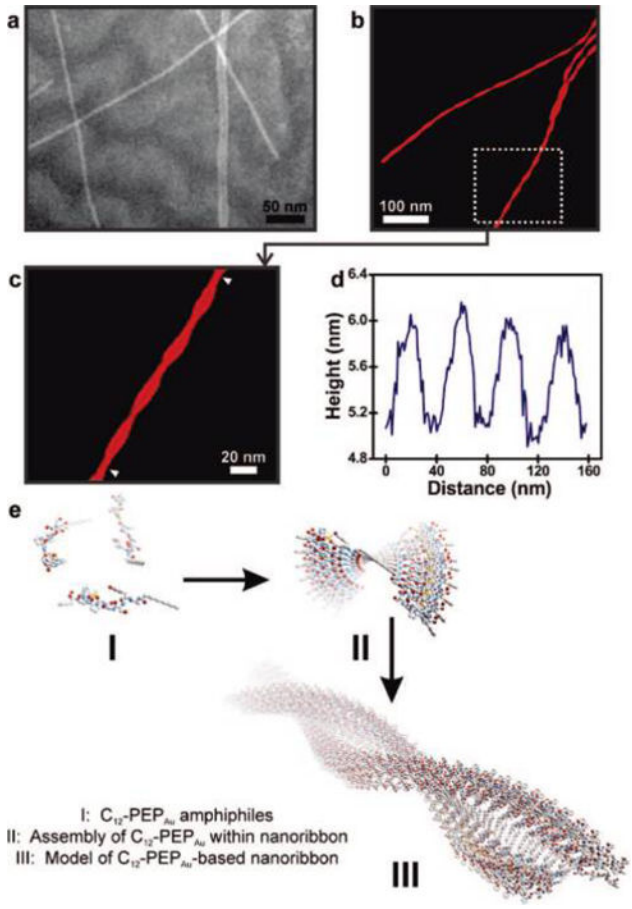

Figure 1.

C_{12}–PEP_{Au} fiber characterization and model of assembly. TEM images reveal that C_{12}–PEP_{Au} amphiphiles assemble into uniform fibers (width = 6.1 ± 0.6 nm; based on 60 counts) in HEPES buffer solutions (a). These fibers have twisted-ribbon morphologies, as evidenced by tapping-mode AFM height images (b,c). The twisted nanoribbons have a regular pitch of 84.1 ± 4.2 nm, as determined by AFM height images (based on 60 counts) (d). C_{12}–PEP_{Au} units assemble into left-handed twisted nanoribbons (e).

Author Manuscript Author Manuscript Author Manuscript Author Manuscript

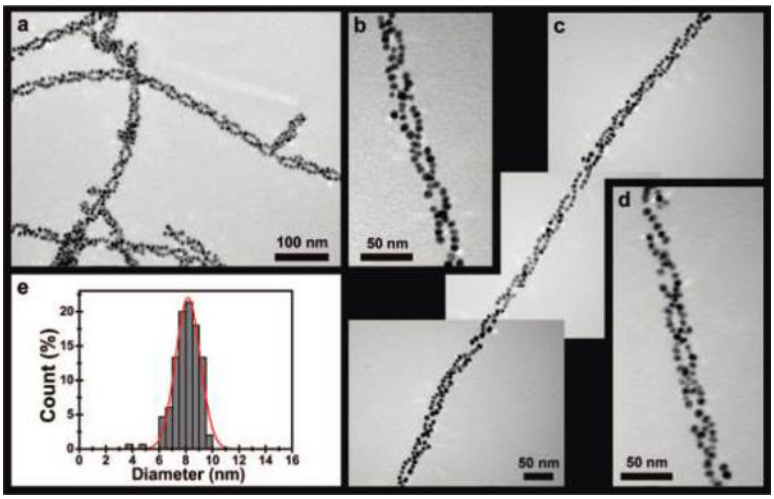

Figure 2.

TEM characterization of gold nanoparticle double helices. Structurally regular gold nanoparticle double helices form when a solution of chloroauric acid is added to HEPES buffer solutions containing C_{12}–PEP_{Au}, as evidenced by TEM analysis (a-d). The sizes of the gold nanoparticles are uniform (8.2 ± 1.0 nm; based on 150 counts) (e).

Author Manuscript Author Manuscript Author Manuscript Author Manuscript

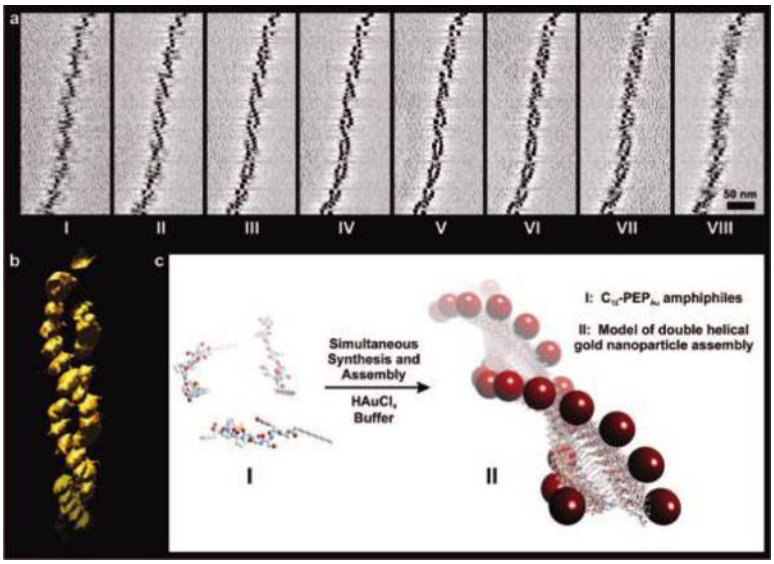

Figure 3.

Electron tomography data (a,b) and schematic depiction of the formation of gold nanoparticle double helices (c). The structure of a gold nanoparticle double helix is confirmed using electron tomography. *X*–*Y* computational slices (a, I–VIII) of the 3-D tomographic volume containing the double helical gold nanoparticle assembly and a 3-D surface rendering of the tomographic volume (b) both reveal the left-handed nature of the helices. Left-handed gold nanoparticle double helices are synthesized and assembled directly in a reaction containing HEPES buffer solutions of chloroauric acid and C_{12}- PEP_{Au} (c).